

# Jiedu Xiaozheng Yin Inhibits the Progression of Colitis Associated Colorectal Cancer by Stimulating Macrophage Polarization Towards an M1 Phenotype via the TLR4 Pathway

Integrative Cancer Therapies  
Volume 23: 1–14  
© The Author(s) 2024  
Article reuse guidelines:  
sagepub.com/journals-permissions  
DOI: 10.1177/15347354241247061  
journals.sagepub.com/home/ict



Haiqin Liu, MMED<sup>1,2,3\*</sup> , Shuo Yan, MMED<sup>1,2,3\*</sup>, Ruiming Yang, MMED<sup>1,2,3</sup>, Caidi Huang, MMED<sup>4,5</sup>, Kangyue Guo, BD<sup>1</sup>, Shi Wang, BD<sup>1</sup>, Yunmei Huang, MMED<sup>1,2,3</sup>, Dongyi Shen, BD<sup>1</sup>, Ying Lin, MD<sup>4,5</sup> , Zhiyun Cao, MD<sup>1,2,3</sup>, Hangan Zhong, MMED<sup>1,6</sup>, Jiumao Lin, MD<sup>1,2,3</sup>, and Xuzheng Chen, MD<sup>1,2,3</sup>

## Abstract

To investigate the effect of Jiedu Xiaozheng Yin (JXY) on the polarization of macrophages in colitis-associated colon cancer (CAC). An orthotopic model of CAC was established to monitor changes in the pathological state of mice. Colon length, number of colon tumors were recorded, and indices for liver, spleen, and thymus were calculated. Hematoxylin and eosin (H&E) staining was employed to observe intestinal mucosal injury and tumor formation. Immunohistochemistry (IHC) staining was utilized to investigate the effect of JXY on M1 and M2 polarization of macrophages in the colonic mucosa of CAC mice. For in vitro experiments, RT-qPCR (Reverse Transcription-quantitative PCR) and flow cytometry were used to observe the effect of JXY on various M1-related molecules such as IL-1 $\beta$ , TNF- $\alpha$ , iNOS, CD80, CD86, and its phagocytic function as well as M2-related molecules including Arg-1, CD206, and IL-10. Subsequently, after antagonizing the TLR4 pathway with antagonists (TAK242, PDTTC, KG501, SRI1302, LY294002), the expression of IL-6, TNF- $\alpha$ , iNOS, and IL-1 $\beta$  mRNA were detected by RT-qPCR. In vivo experiments, the results showed that JXY improved the pathological condition of mice in general. And JXY treatment decreased the shortening of colon length and number of tumors as compared to non-treated CAC mice. Additionally, JXY treatment improved the lesions in the colonic tissue and induced a polarization of intestinal mucosal macrophages towards the M1 phenotype, while inhibiting polarization towards the M2 phenotype. In vitro experiments further confirmed that JXY treatment promoted the activation of macrophages towards the M1 phenotype, leading to increased expression of IL-1 $\beta$ , TNF- $\alpha$ , iNOS, CD80, CD86, as well as enhanced phagocytic function. JXY treatment concomitantly inhibited the expression of M2-phenotype related molecules Arginase-1 (Arg-1), CD206, and IL-10. Furthermore, JXY inhibited M1-related molecules such as IL-6, TNF- $\alpha$ , iNOS, and IL-1 $\beta$  after antagonizing the TLR4 pathway. Obviously, JXY could exhibit inhibitory effects on the development of colon tumors in mice with CAC by promoting M1 polarization through TLR4-mediated signaling and impeding M2 polarization of macrophages.

## Keywords

Jiedu Xiaozheng Yin, colitis associated colon cancer, RAW264.7, macrophage polarization, TLR4

Submitted September 15, 2023; revised February 4, 2024; accepted March 28, 2024

## Introduction

Colorectal Cancer (CRC) is the third most commonly diagnosed cancer and the second leading cause of cancer-related

deaths globally.<sup>1</sup> Colitis-associated colon cancer (CAC), which falls under the category of CRC, exhibits greater malignancy and poses greater challenges in terms of treatment compared to sporadic colon cancer.<sup>2</sup> Consequently, it is



Creative Commons Non Commercial CC BY-NC: This article is distributed under the terms of the Creative Commons Attribution-NonCommercial 4.0 License (<https://creativecommons.org/licenses/by-nc/4.0/>) which permits non-commercial use, reproduction and distribution of the work without further permission provided the original work is attributed as specified on the SAGE and Open Access pages (<https://us.sagepub.com/en-us/nam/open-access-at-sage>).

imperative for physician scientists to actively pursue rational and efficacious strategies for the prevention and management of CAC. In comparison to conventional surgical excision, radiotherapy, chemotherapy, and other therapeutic modalities, traditional Chinese medicine (TCM) has garnered significant interest owing to its numerous advantages, including its multi-component nature, ability to target multiple sites, minimal side effects, and remarkable efficacy.<sup>3</sup>

Jiedu Xiaozheng Yin (JXY), a TCM compound, exhibits heat-clearing, detoxifying, tumor-shrinking properties, and demonstrates exceptional anti-tumor effects.<sup>4</sup> Previous research has demonstrated that JXY effectively hinders the development of blood vessels and lymphatic vessels associated with cancer through the VEGF-C/VEGFR-3 pathway,<sup>5</sup> while also inducing tumor cell apoptosis via a mitochondria-mediated pathway.<sup>6-8</sup> JXY has been shown to reverse drug resistance in cancer stem cells induced by fluorouracil, thereby enhancing the anti-tumor effects of fluorouracil.<sup>9,10</sup> Additionally, JXY also has the ability to regulate glucose energy metabolism through the HIF-1/miR-210 pathway, resulting in the inhibition of tumor cell proliferation.<sup>11</sup>

Macrophages are a subset of innate immune cells that typically exist in 2 distinct subpopulations. The first subpopulation, known as classically activated or M1 macrophages, exhibit pro-inflammatory properties and are stimulated by lipopolysaccharide (LPS) alone or in combination with Th1 cytokines (eg, IFN- $\gamma$ , GM-CSF). These M1 macrophages produce various pro-inflammatory cytokines, including interleukin (IL)-1 $\beta$ , IL-6, IL-12, IL-23, and TNF- $\alpha$ . The second subpopulation, referred to as M2 macrophages, possess anti-inflammatory and immunoregulatory capabilities. These M2 macrophages are polarized by Th2 cytokines such as IL-4 and IL-13, and they produce anti-inflammatory cytokines such as IL-10 and TGF- $\beta$ .<sup>12,13</sup> Tumor-associated macrophages (TAMs) is a population of macrophages that exhibit M2-like characteristics, which are highly abundant and actively infiltrating inflammatory cells within the tumor microenvironment (TME), exert a pivotal influence on CRC. TAMs engage in interactions with tumor cells through the release of exosomes and various cytokines, thereby facilitating tumor cell proliferation, invasion, migration, and angiogenesis. Additionally, TAMs possess the ability to modulate adaptive immunity and

facilitate immune evasion by tumors.<sup>14,15</sup> Presently, it is established that the Toll-like receptor 4 (TLR4) and IL-4 receptor (IL-4R) pathways are intimately associated with macrophage polarization and play a critical role in regulating macrophage polarization.<sup>16,17</sup>

Macrophage polarization is closely related to tumor development. Consequently, the active pursuit of pharmaceutical interventions capable of regulating macrophage polarization to effectively combat CAC would greatly benefit patients. This study aims to explore the effect of JXY on macrophage polarization during the progression of CAC and clarify the underlying anti-tumor molecular mechanisms. Our findings demonstrate that JXY facilitates the promotion of M1-phenotype polarization via the TLR4 pathway, while simultaneously inhibiting M2-phenotype polarization. These results substantiate the potential candidacy of JXY as a therapeutic agent for CAC treatment.

## Materials and Methods

### Materials and Reagents

The mouse macrophage cell line RAW264.7 was purchased from the Cell Bank of the Chinese Academy of Sciences (Shanghai, China). High-glucose DMEM medium (11965092) and fetal bovine serum (10100147) were purchased from Gibco (Grand Island, USA). A total RNA extraction kit (BSC52M1) was obtained from Bori Biotech Co., Ltd. (Anhui, China). A reverse transcription kit (RR047A) and fluorescent quantitative PCR reagent (RR420A) were purchased from Takara (Kyoto, Japan). A cell Counting Kit (CCK-8, FC101-02) was obtained from TransGen Biotech Co., Ltd. (Beijing, China). CD80 (11-0801-82), CD86 (25-0862-82) were purchased from Thermo Fisher (MA, USA). Tetramethylrhodamine isothiocyanate (TRITC Dextran, T1162) was purchased from Merck (NY, USA). Azoxymethane (AOM, A5486) was purchased from Sigma (MO, USA). Dextran sulfate sodium (DSS, 216011090) was obtained from MP Biomedicals (CA, USA). An immunohistochemical antibody kit (97624T) was obtained from Cell Signaling Technology (MA, USA). TAK-242 (A3850), PDTC (B6422), KG-501 (B8380), SR11302 (A8185), and LY294002 (A8250) were purchased from APExBio (Houston, USA).

<sup>1</sup>Academy of Integrative Medicine, Fujian University of Traditional Chinese Medicine, Fuzhou, China

<sup>2</sup>Fujian Key Laboratory of Integrative Medicine on Geriatrics, Fuzhou, China

<sup>3</sup>College of Integrative Medicine, Fujian Province University, Fuzhou, China

<sup>4</sup>The Shengli Clinical Medical College, Fujian Medical University, Fuzhou, China

<sup>5</sup>Department of Pathology, Fujian Provincial Hospital, Fuzhou, China

<sup>6</sup>Shanghang Hospital of Traditional Chinese Medicine, Longyan, China

\*These authors contributed equally to this work.

### Corresponding Author:

Xuzheng Chen, Academy of Integrative Medicine, Fujian University of Traditional Chinese Medicine, 1 Qiuyang Road, Minhou Shangjie, Fuzhou 350122, China.

Email: 471235814@qq.com

### JXY Preparation

Hedyotis diffusa Willd (30 g), Spica prunellae (15 g), Pseudobulbus Cremastrae (15 g), and Sophora Flavescens (15 g) were purchased from Guo Yi Tang Hospital of Fujian University of Traditional Chinese Medicine (Fuzhou, China). For the in vitro experiments, the herbs were extracted by reflux with ethanol twice, decompressed and concentrated. Then the concentrate was extracted with ethyl acetate thrice.<sup>18</sup> For the in vivo experiments, the herbs were extracted with water twice and concentrated.

### Animals

AOM and DSS were used to construct a male BALB/c mouse model of CAC. The mice were initially randomly divided into four groups based on body weight ( $n=7$ /per group): control group (Cont), Model group (Model), Model + JXY group (Model + JXY), JXY alone group (JXY). The Model and Model + JXY mice were administered 12.5 mg/kg AOM. Following a week, the mice were provided with drinking water supplemented with 2.5% DSS for 6 days. This treatment was repeated twice more after a 2-week recovery period. Subsequent to the first round of DSS administration, the Model + JXY and JXY mice were orally administered JXY (7.5 g/kg). The Cont group and Model group mice were injected with an equal volume of saline. Animal samples were collected on the 68th day of the experiment. All animal experiments were conducted in accordance with the national guidelines for the humane treatment of animals and were approved by the Ethics Committee of Fujian University of Traditional Chinese Medicine (FJTCMIACUC 2022006).

### Physiological State of Mice

The mice were subjected to monitoring of various general conditions, such as weight, fecal occult blood, and diarrhea. Additionally, the disease activity index (DAI) was determined using the formula:  $\text{DAI} = \text{weight loss score} + \text{fecal occult blood score} + \text{diarrhea index}$ , with the specific scoring criteria provided in the Supplemental Data (Table SI-III). The liver, spleen, and thymus of mice were weighed. According to the formula:  $\text{organ index} = (\text{organ weight} / \text{mouse weight}) \times 100$ , the liver index, spleen index, and thymus index of mice were calculated. The colon was cut from the upper end of the cecum to the end of the anus, and the length was measured and photographed. Afterwards, the colon was dissected longitudinally to observe whether there were visible tumors in the colon. The number of tumors raised on the surface of the colon was recorded. Then, colon tissues were fixed with a 4% paraformaldehyde solution for subsequent H&E and Immunohistochemistry (IHC).

### H&E Staining

First, the embedded wax tissue was cut into 4  $\mu\text{m}$  slices and baked in the oven at 60°C for 2 hours. Then the tissue was dewaxed and rehydrated. After the hematoxylin staining, eosin staining was performed. Finally, the tissue was air-dried and sealed with neutral resin, and histopathological conditions were observed under an inverted microscope (Leica, Solms, Germany). Random fields of each section were imaged at a magnification of 100 $\times$  and 200 $\times$ .

### IHC Analysis

The tissue, as described above, was observed by immunohistochemistry (IHC). Firstly, primary antibodies F4/80 (1:300), CD68 (1:500), IBa1 (1:200), CD86 (1:300), CD11c (1:500), CD206 (1:500), and Arg-1 (1:150) were diluted proportionally and then added to the tumor tissue slices. Slices were incubated overnight in a wet box at 4°C. Then a biotinylated secondary antibody was added and incubated for 1 hours. Streptomyacin peroxidase was added to the tissues and incubated at RT for about 10 minutes. Finally, the slices were stained with DAB and hematoxylin. Neutral resin was used to seal the slices. Random fields of each section were imaged at a magnification of 400 $\times$  by a microscope.

### Cell Culture

RAW264.7 cells were cultured with high-glucose DMEM medium containing 10% fetal bovine serum, and 1 % penicillin-streptomycin at 37°C in a 5% CO<sub>2</sub> humidified incubator. The cells were frozen during the logarithmic growth phase.

### CCK-8 Assay

RAW264.7 cells were inoculated into 96-well plates and treated with different doses of JXY (50, 100, 200, and 400  $\mu\text{g/mL}$ ) for 24, 48, and 72 hours respectively. CCK-8 reagent was then added to each well (100  $\mu\text{L}$ /well) and incubated for 2 hours. The absorbance was measured at 450 nm via an ELX800 microplate reader (BioTek Instruments, Inc., Winooski, VT, USA).

### Observation of Morphological Changes

RAW264.7 cells with a density of  $3 \times 10^5$  cells/mL were inoculated into a 6-well culture plate. The Cont group (no intervention), the LPS group (500 ng/mL LPS intervention for 6 hours), and the JXY group (50  $\mu\text{g/mL}$  JXY intervention for 6 hours) were set up. The morphology of RAW264.7 cells were observed using a phase-contrast microscope at 200 $\times$ .

**Table 1.** Real Time PCR Primer Sequence.

| Gene          | Primer | Sequence (5'-3')         |
|---------------|--------|--------------------------|
| IL-1 $\beta$  | F      | GCCTCGTGCTGTCGGACCCATAT  |
|               | R      | TCCTTTGAGGCCCAAGGCCACA   |
| IL-6          | F      | CTGCAAGAGACTTCCATCCAG    |
|               | R      | AGTGGTATAGACAGGTCTGTTGG  |
| TNF- $\alpha$ | F      | GAGTGACAAGCCTGTAGCC      |
|               | R      | CTCCTGGTATGAGATAGCAAA    |
| iNOS          | F      | CACCAAGCTGAACTTGAGCG     |
|               | R      | CGTGGCTTTGGGCTCCTC       |
| CD206         | F      | TGCCACCAATCACAACATACAC   |
|               | R      | ACAGGTCGCCTTGAAGTGTT     |
| IL-10         | F      | CCTGGGTGAGAAGCTGAAGAC    |
|               | R      | CTTGTAGACACCTTGGTCTTGG   |
| Arg-1         | F      | CAGCAGAGGAGGTGAAGAGTA    |
|               | R      | TAGTCAGTCCCTGGCTTATGG    |
|               | F      | ACGGCAAGTTCAACGGCACAG    |
| GAPDH         | R      | GAAGACGCCAGTAGACTCCACGAC |

### Reverse Transcription-Quantitative PCR (RT-qPCR)

RAW264.7 cells were inoculated into a 6-well culture plate with a density of  $1 \times 10^5$  cells/mL and divided into the Cont group and JXY group. After cell adhesion, the JXY cells were treated with 50  $\mu$ g/mL JXY for 6 hours, and then harvested. The transcription levels of IL-1 $\beta$ , iNOS, and TNF- $\alpha$  mRNA were analyzed. RAW264.7 cells were inoculated into a 6-well culture plate with  $1 \times 10^5$  cells/mL and divided into cont group, IL-4 group, IL-4 + JXY group, and JXY group. After cell adhesion, the IL-4 + JXY group cells were preincubated with 50  $\mu$ g/mL JXY for 1 hour, and then 20 ng/mL IL-4 was added for 6 hours. The IL-4 group cells and the JXY group cells were given the same dose of IL-4 and JXY for intervention, respectively. The expression of Arginase-1 (Arg-1), CD206, and IL-10 mRNA were detected by RT-qPCR. First, total RNA was extracted and its concentration was detected. Then RNA was reverse-transcribed into cDNA. Finally cDNA was amplified in a fluorescent quantitative PCR apparatus (Applied Biosystems, Inc., CA, USA) under the following conditions: 95°C, 30 s, 40 cycles: 95°C, 5 s; 60°C, 30 s. The relative quantification of the target genes was carried out by the  $2^{-\Delta\Delta C_t}$  method, and GAPDH was used as the internal control. The primer sequences are listed in Table 1.

### Co-Culture Experiments

RAW264.7 cells were inoculated at  $1 \times 10^5$  cells/mL into a 6-well culture plate. After the cells adhered to the plate, the supernatant was removed and replaced with the supernatant of CT26 cells for 5 days. The experiment was divided into Cont group (no intervention), the supernatant of CT26

group (SQ, RAW264.7 cells were cultured with the supernatant of CT26 cells), the supernatant of CT26 + JXY group (SQ + JXY, RAW264.7 cells were cultured with the supernatant of CT26 cells and treated with JXY). Before collecting samples, 50  $\mu$ g/mL JXY was added to the SQ + JXY group cells for 6 hours. Finally, the expression of Arg-1, CD206, and IL-10 mRNA were detected.

### Flow Cytometry

RAW264.7 cells were inoculated at  $1 \times 10^5$  cells/mL into a 6-well culture plate and were divided into the Cont group and JXY group. After the cells adhered to the plate, the JXY group cells were added with JXY at a concentration of 50  $\mu$ g/mL for 24 hours. Then, the density of cell suspensions was adjusted to  $1 \times 10^6$  cells/mL and moved into falcon tubes (352052, BD, MA, USA). 1  $\mu$ g CD80-FITC or 1  $\mu$ g CD86-PE-Cy7 was added to the tubes. The tubes were incubated at RT and away from light for 20 minutes. Then 1 mL of PBS was added to each tube and centrifuged twice for 5 minutes at 1000 rpm. Finally, the fluorescence intensity of FITC or PE-Cy7 was detected by a flow cytometer (FACSCelesta, BD, MA, USA) with 400  $\mu$ L PBS cell suspension.

### Phagocytic Experiments

As mentioned above, after the RAW264.7 cells were divided into the JXY group and Cont group, the JXY group cells were incubated with 50  $\mu$ g/mL JXY for 12 hours. The 2 group cells were incubated with 300  $\mu$ g/mL TRITC Dextran at 37°C in an atmosphere containing 5% CO<sub>2</sub> for 30 minutes. Finally, the fluorescence intensity of TRITC was measured by flow cytometry.

### Statistical Analysis

The data were analyzed by SPSS 22.0 software. All data were expressed as mean  $\pm$  standard deviation (SD). Statistical analyses of the data were performed with repeated measures analysis of variance or Student's *t*-test.  $P < .05$  was considered statistically significant.

## Results

### JXY Inhibits Tumor Formation in CAC Mice

The method of animal modeling is shown in Figure 1A. Compared with the Cont group, the mice in the model group showed weight loss, diarrhea, fecal occult blood, an increased DAI index, a shortened colon length, a thickened lumen and the development of tumors. Compared with the Model mice, the Model + JXY mice demonstrated alleviation of weight loss, diarrhea, and fecal occult blood, along with an improvement in the DAI index. Through the comparison of various



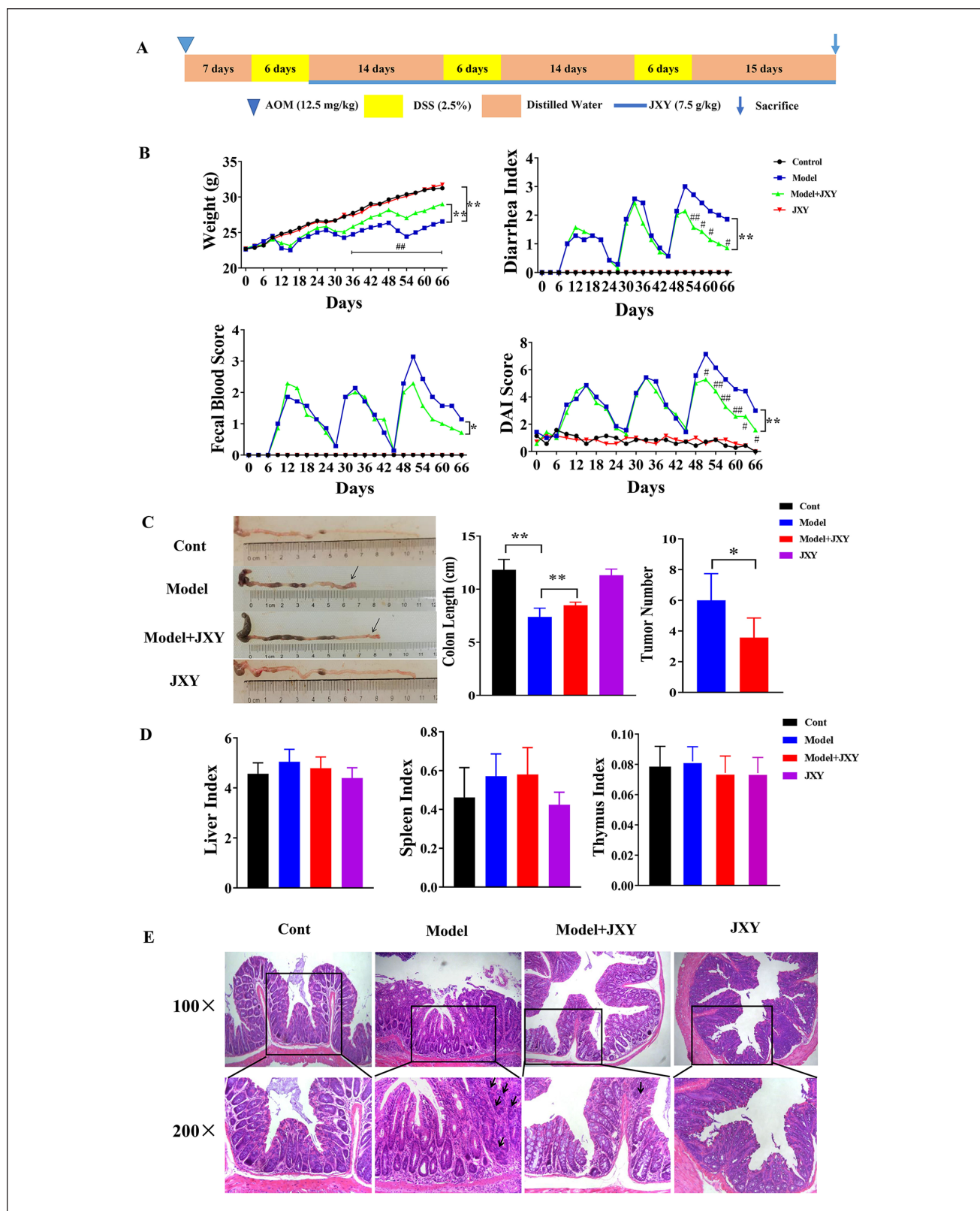


**Figure 1.** Effect of JXY on CAC mice induced by AOM/DSS. (A) Schematic diagram of CAC mouse model induced by AOM/DSS. (B) Effect of JXY on body weight, diarrhea, fecal occult blood and DAI index in mice. (C) Effect of JXY on colon length and tumor number in mice. (D) Effect of JXY on liver, spleen and thymus index in mice. (E) Effect of JXY on colon histopathology in mice. The black arrow represents colon tumors (100×, 200×), \* $P < .05$ , \*\* $P < .01$ . Compared with the Model group, # $P < .05$ , ## $P < .01$ .

time points, it was found that, compared with the Model group, the weight of the Model+JXY group showed significant weight recovery on day 36 and after. The diarrhea index improved on days 54 to 60 and 66, DAI score also improved on days 51 to 66, as illustrated in Figure 1B. Furthermore, the Model+JXY mice experienced relief from the shortened colon length and thickened lumen, and a reduction in the number of tumors (indicated by black arrows), as shown in Figure 1C. JXY did not demonstrate any notable impact on the liver, spleen, or thymus index of CAC mice, as evidenced by the findings presented in Figure 1D. The results of H&E staining showed that the colonic structure of both the Cont and JXY mice were remained intact, with well-organized villi, abundant goblet cells, and an absence of inflammatory cell infiltration. Conversely, the Model mice exhibited numerous colon tumors (indicated by the black arrows). The crypt structure and goblet cells of the colon disappeared, while atypical cell proliferation was evident, characterized by significantly enlarged, deeply stained nuclei displaying atypical features. In comparison to the mice in the Model group, the mice in the Model+JXY group exhibited a reduced level of tumor infiltration and an improvement in the disorder of colon cell arrangement, inflammatory cell infiltration. The findings presented in Figure 1E provide confirmation that JXY has the ability to ameliorate the histopathological alterations in the colon of CAC mice induced by AOM/DSS.

### *JXY Promotes M1-Type Macrophage Polarization and Inhibits the Formation of TAMs in the CAC Mouse*

In order to investigate the effect of JXY on the polarization of macrophages in the CAC mouse, the levels of total macrophage markers, including G-protein-coupled receptor (F4/80), macrophage sialic acid protein (CD68), and Ionic calcium binding adapter molecule (IBA1), were initially examined (Figure 2A). It was found that the expression of F4/80, CD68, and IBA1 was relatively low in both the Cont group and JXY group. Conversely, in the Model group, there was a significant increase in the expression of these markers in the colon mucosa and lamina propria. The intervention of JXY demonstrated a significant reduction in the infiltration of macrophages in the intestinal mucosa and lamina propria. These findings indicate that JXY has the potential to mitigate colon inflammation in mice with CAC. Subsequently, the M2 macrophage-related molecules CD206 and Arg-1 were observed (Figure 2B). The expression of CD206 was found to be low in both the control and JXY-treated mice, while Arg-1 was not detected in either group. These results suggest a diminished presence of M2 macrophages in the intestinal mucosa in the absence of inflammation. However, the expression of CD206 and Arg-1 in the tumor tissue of the Model group exhibited a

significant increase, which was effectively reduced by the administration of JXY. Furthermore, the expression of CD86 and CD11c in M1 phenotype macrophages were examined. In both the control and JXY-treated mice, the expression levels of CD11c and CD86 were found to be low and scattered in the mucosa and lamina propria. Notably, the expression levels of CD11c and CD86 showed a tendency to increase in the model mice, but were significantly elevated following JXY intervention, suggesting that JXY facilitates the infiltration of M1 phenotype macrophages (Figure 2C). These data showed that JXY promotes M1-phenotype macrophage polarization and inhibits the formation of TAMs in the CAC mouse.

### *JXY Promotes M1-type Polarization of RAW264.7 Macrophages In Vitro*

RAW264.7 cells were subjected to treatment with JXY at various concentrations (0, 50, 100, 200, and 400  $\mu\text{g/mL}$ ) for 24, 48, and 72 hours. It was observed that JXY, at concentrations exceeding 100  $\mu\text{g/mL}$ , exhibited a significant dose-dependent inhibition of RAW264.7 cell growth. Conversely, concentrations below 50  $\mu\text{g/mL}$  did not demonstrate any significant inhibitory effect on cell growth at any of the observed time points (24, 48, or 72 hours). Consequently, a concentration of 50  $\mu\text{g/mL}$  of JXY was chosen for subsequent experiments in this study, as shown in Figure 3A. In the normal state, RAW264.7 cells exhibited a round, small morphology and grew in clusters. Following a 6-hour intervention with JXY, the cells displayed enlarged size and diverse morphologies. Notably, certain cells exhibited protrusions and spindle-like growth (as indicated by arrows). This change resembled the observations made in the positive control LPS group, as shown in Figure 3B. The expression of IL-1 $\beta$ , TNF- $\alpha$ , and iNOS in M1-type macrophages were detected by RT-qPCR. Subsequent to the JXY intervention, there was a significant increase in the expression of M1-phenotype associated molecules IL-1 $\beta$ , TNF- $\alpha$ , and iNOS, as shown in Figure 3C. Flow cytometry was employed to assess the expression of M1-phenotype macrophage-related molecules CD80 and CD86 in each experimental group. Following JXY intervention, a notable increase in the fluorescence intensity of CD86 in macrophages was observed, while the fluorescence intensity of CD80 remained unchanged, as depicted in Figure 3D. Additionally, flow cytometry was utilized to evaluate the phagocytic capability of cells through TRITC-Dextran engulfment. The findings demonstrated a significant enhancement in the fluorescence intensity of TRITC-Dextran subsequent to JXY intervention, providing evidence that JXY enhances the phagocytic function of RAW264.7 cells, as illustrated in Figure 3E. The data indicates that JXY promotes M1-phenotype polarization of RAW264.7 cells.



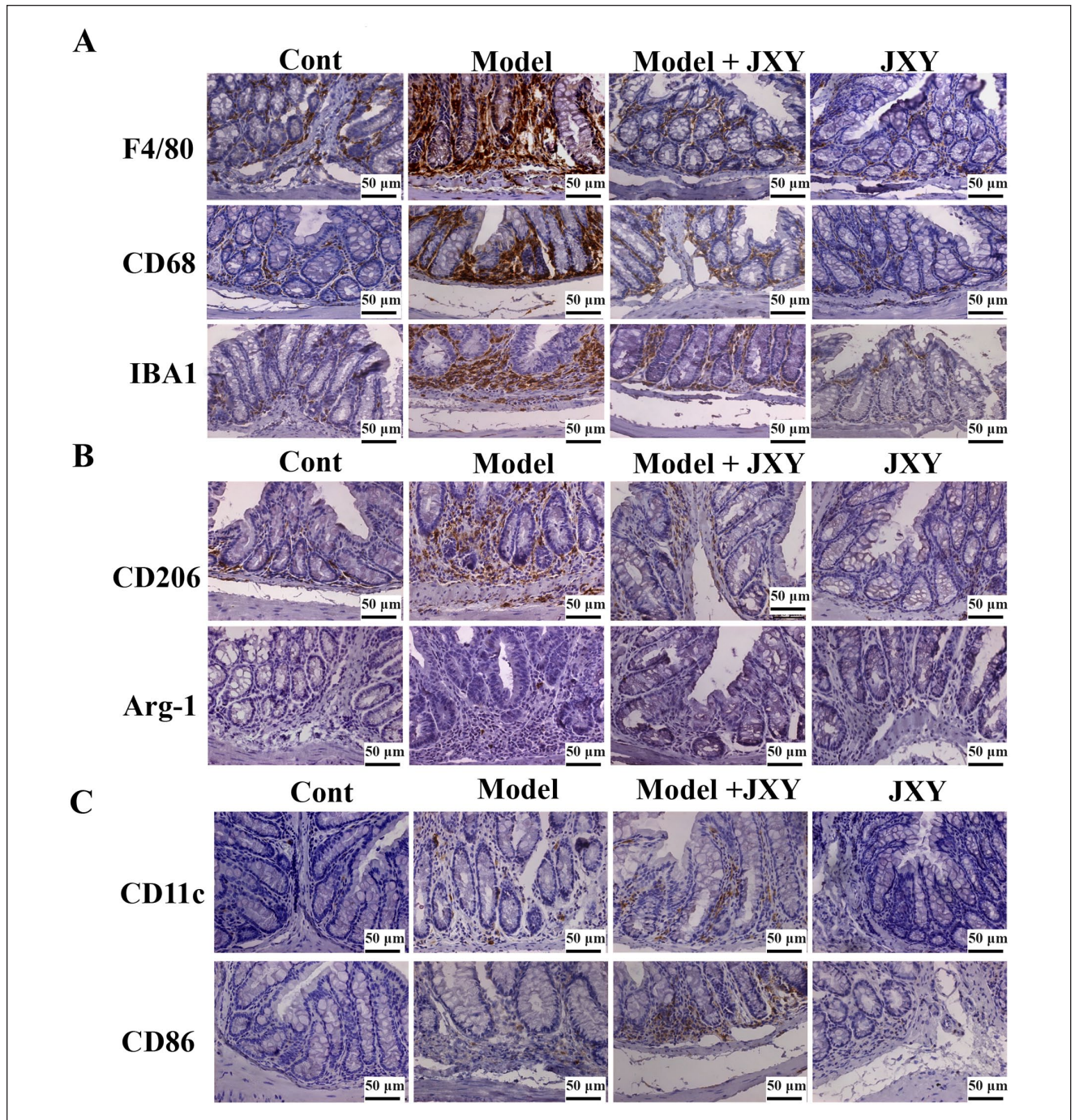


**Figure 2.** Effect of JXY on related molecules of M1 and M2 macrophages. (A) Effect of JXY on the expression of F4/80, CD68 and IBA1 in colon tissue of mice (400 $\times$ ). (B) Effect of JXY on the expression of CD206 and Arg-1 in colon tissue of mice (400 $\times$ ). (C) Effect of JXY on the expression of CD86 and CD11c in colon tissue of mice (400 $\times$ ).

### JXY Inhibits M2-type Polarization of RAW264.7 Cells

In order to investigate the effect of JXY on the polarization of M2 macrophages, the present study employed IL-4 as an inducer for M2-phenotype polarization of macrophages. The

potential antagonistic effect of JXY on IL-4 signaling was observed. The mRNA expression of Arg-1, CD206, and IL-10 were detected by RT-qPCR after JXY intervention in RAW264.7 cells activated by IL-4. The results revealed a significant increase in the mRNA levels of Arg-1, CD206, and IL-10 in IL-4-treated cells compared to control cells. These increases

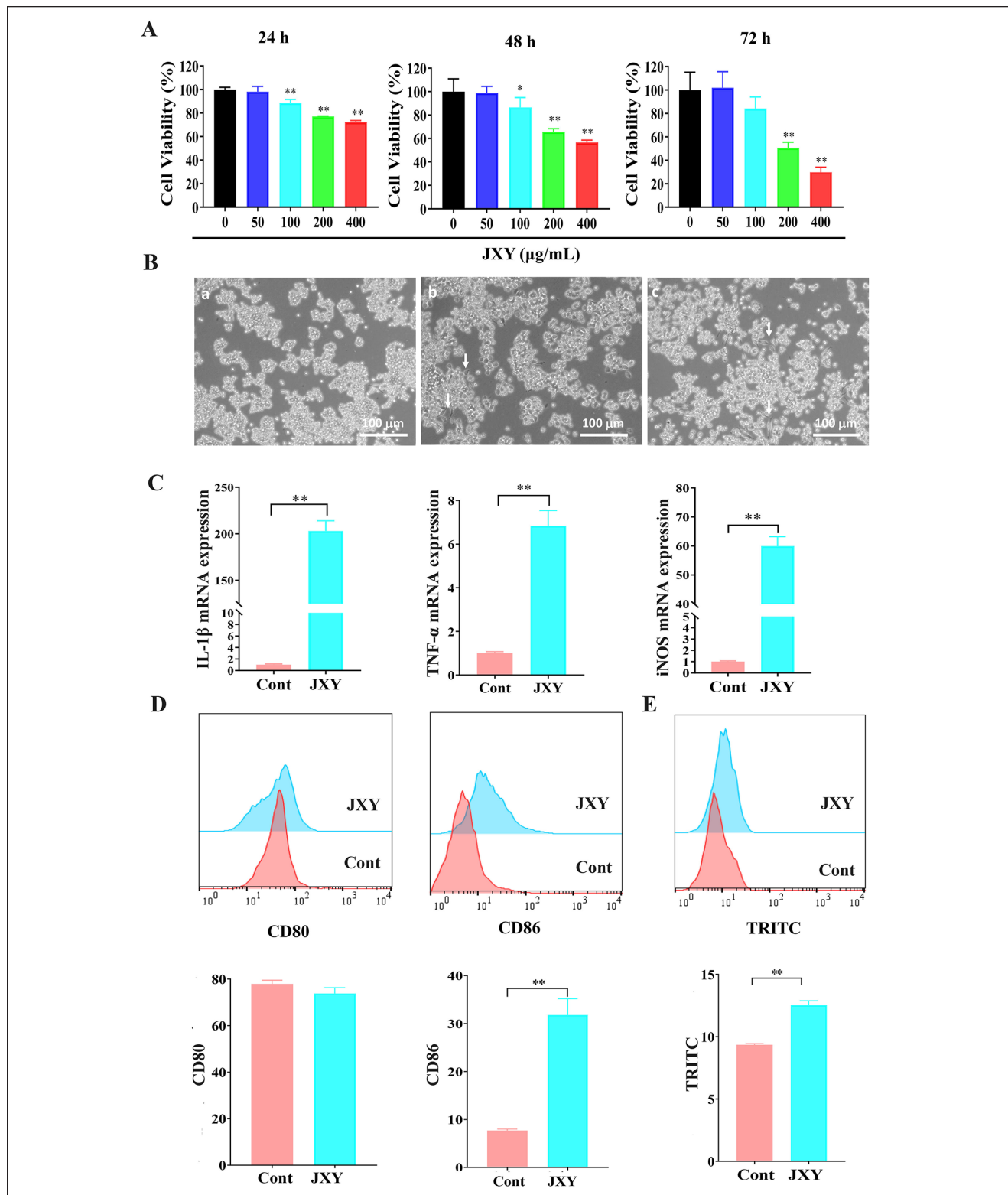


**Figure 3.** JXY promotes the M1 phenotype polarization of RAW264.7 cells. (A) Effect of JXY on viability rate of RAW264.7 cells. Compared with 0 µg/mL group, \* $P < .05$ , \*\* $P < .01$ . (B) Effect of JXY on morphology of RAW264.7 cells (200 $\times$ ). Upon stimulation with LPS or JXY, RAW264.7 cells exhibited significant morphological changes characterized by increased cell size and, including the protrusion of pseudopodia and elongation into spindle-like structures. (indicated by the white arrows). Cont group (a); LPS group (b); JXY group (c). (C) Effect of JXY on the expression of IL-1 $\beta$ , TNF- $\alpha$  and iNOS in RAW264.7 cells, \*\* $P < .01$ . (D) Effect of JXY on the expression of CD80 and CD86 in RAW264.7 cells, \*\* $P < .01$ . (E) Effect of JXY on phagocytosis of RAW264.7 cells, \*\* $P < .01$ .



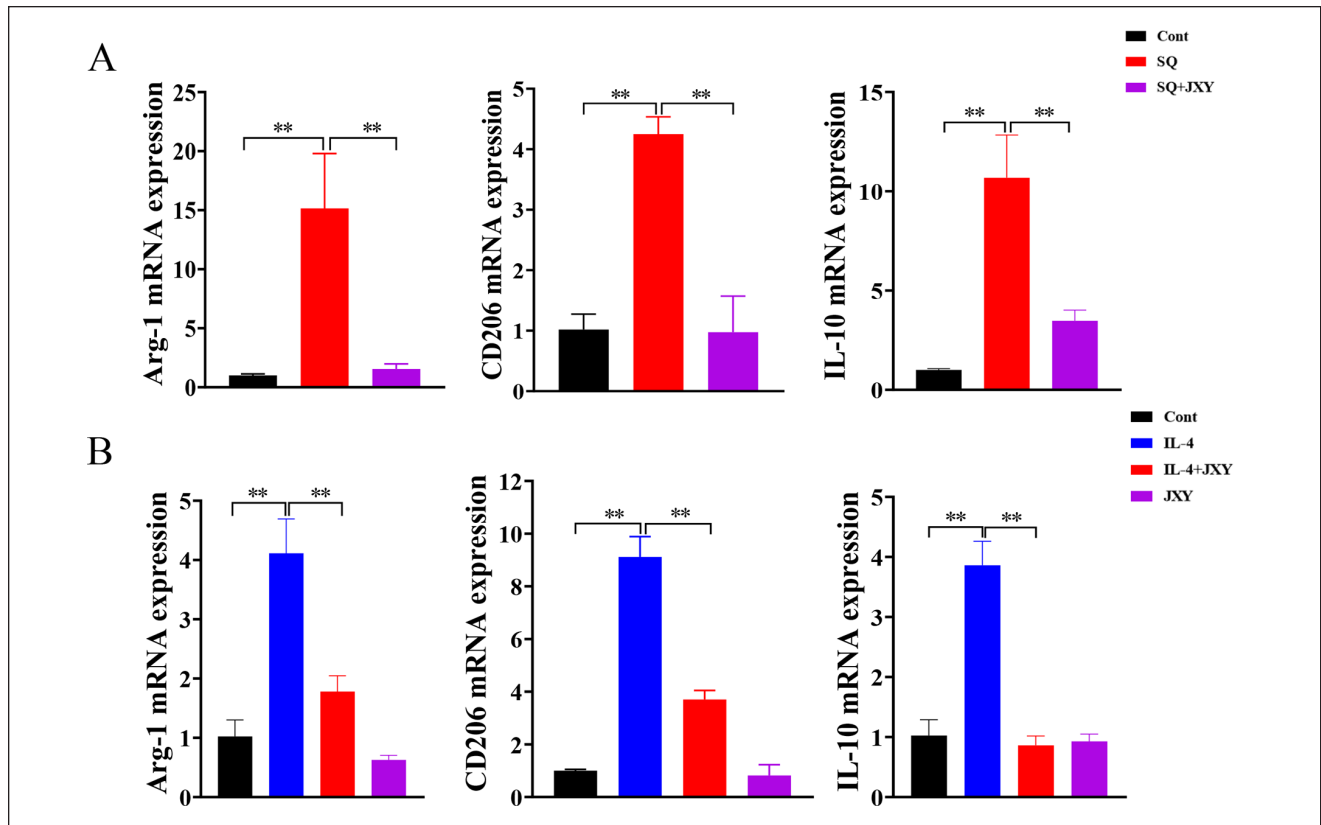


**Figure 4.** JXY inhibits the M2 phenotype polarization of RAW264.7 cells. (A) Effect of JXY on the expression of Arg-1, IL-10 and CD206 in TAMs. SQ, RAW264.7 cells were cultured with the supernatant of CT26 cells. (B) Effect of JXY on the expression of M2 phenotype macrophage related molecules Arg-1, CD206 and IL-10 induced by IL-4. \*\* $p < .01$ .

were significantly inhibited in the IL-4 + JXY cells. It can be concluded that JXY has an antagonistic effect on IL-4 induced macrophage polarization towards the M2 phenotype, and the results are shown in Figure 4A. In addition, there are many TAMs in TME, most of which have M2-phenotype polarization characteristics. To explore the effect of JXY on TAMs, this study cultured RAW264.7 macrophages with the supernatant of CT26 cells to induce TAMs. The expression of Arg-1, IL-10, and CD206 mRNA of RAW264.7 cells was detected by RT-qPCR. Arg-1, CD206, and IL-10 mRNA in the SQ group cells were significantly increased compared with the Cont group cells. After the intervention of JXY, they decreased significantly. Thus, JXY inhibits the expression of M2-phenotype related molecules in TAMs, and the results are shown in Figure 4B. Obviously, JXY inhibits the M2-phenotype polarization of RAW264.7 cells.

#### JXY Promotes M1-Phenotype Polarization of Macrophages Through the TLR4 Pathway

To investigate whether JXY promotes M1-phenotype polarization of RAW264.7 macrophages is related to TLR4 and its downstream NF- $\kappa$ B, MAPK, and PI3K/Akt pathways,

RAW264.7 cells were pre-incubated with 10  $\mu$ M TAK-242 (TLR4 antagonist), PDTC (NF- $\kappa$ B antagonist), KG501 (MAPK/CREB antagonist), SR11302 (MAPK/AP-1 antagonist), or LY294002 (PI3K antagonist) for 1 hour respectively. The expression of IL-6, TNF- $\alpha$ , iNOS, and IL-1 $\beta$  mRNA in RAW264.7 macrophages were detected by RT-qPCR after the intervention of JXY with concentration of 50  $\mu$ g/mL for 6 hours. In comparison to JXY cells, the expression levels of IL-6, TNF- $\alpha$ , iNOS, and IL-1 $\beta$  were significantly reduced following treatment with TAK-242. These findings indicate that JXY facilitates the polarization of M1 macrophages through the TLR4 pathway, as depicted in Figure 5A. Similarly, the expression levels of IL-6, TNF- $\alpha$ , iNOS, and IL-1 $\beta$  were also diminished upon administration of PDTC. This provides evidence that JXY promotes M1 macrophage polarization via the NF- $\kappa$ B pathway, as illustrated in Figure 5B. The application of KG501 resulted in a significant decrease of JXY-induced the expression of IL-6, TNF- $\alpha$ , iNOS, and IL-1 $\beta$ , indicating that JXY facilitates M1 macrophage polarization through regulation of the MAPK/CREB pathway, as depicted in Figure 5C. The use of SR11302 led to a significant decrease of JXY-induced the expression of TNF- $\alpha$ , iNOS, and IL-1 $\beta$ , suggesting that JXY

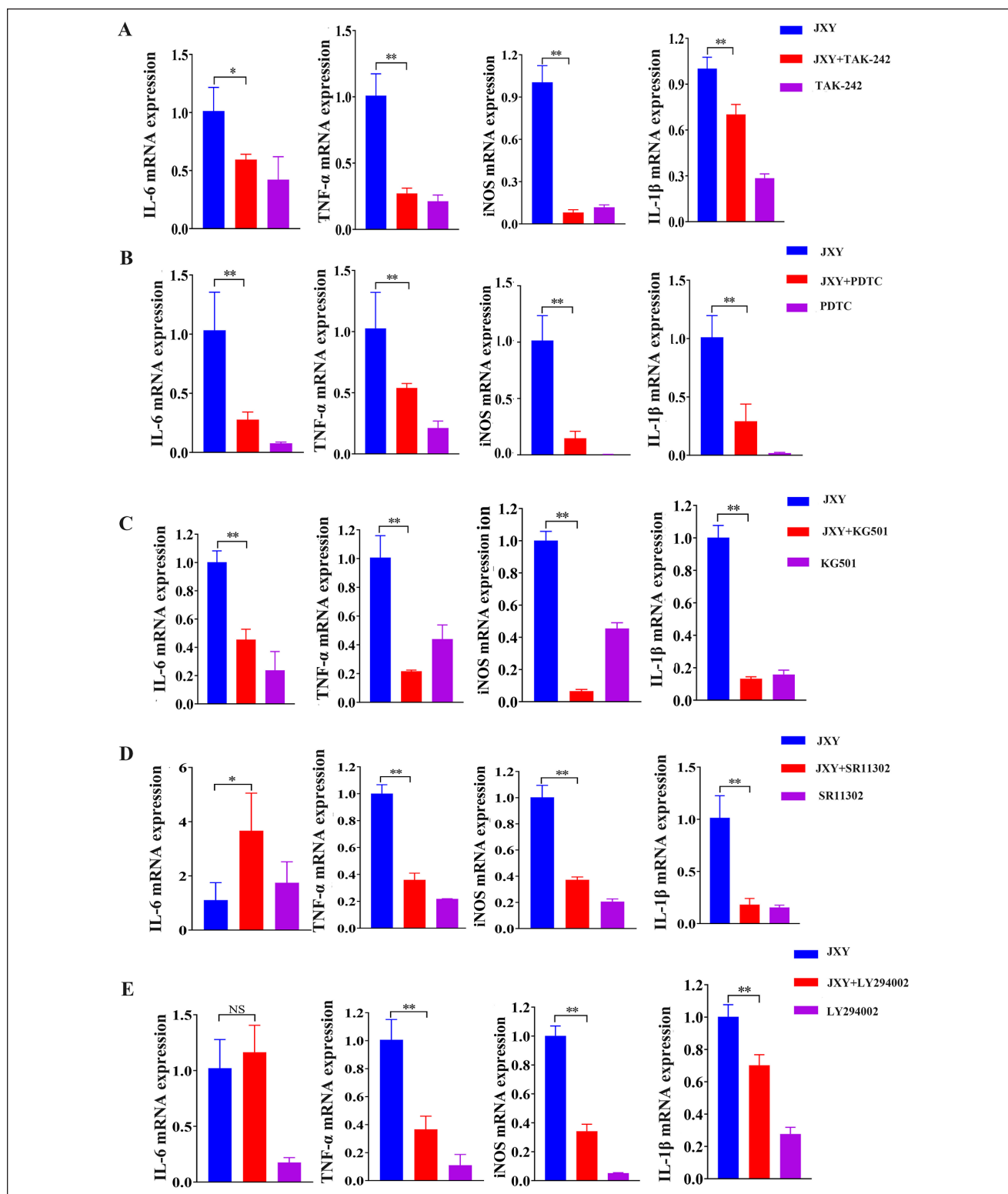


**Figure 5.** JXY promotes M1 phenotype polarization of macrophages through the TLR4 pathway. RAW264.7 cells were pre-incubated with TAK-242 (A), PDTC (B), KG501 (C), SR11302 (D), or LY294002 (E) for 1 hour, then treated with JXY for 6 hours. The expression of IL-6, TNF- $\alpha$ , iNOS and IL-1 $\beta$  mRNA induced by JXY were detected by RT-qPCR.

Abbreviation: NS, no significance.

\* $P < .05$ . \*\* $P < .01$ .

promotes M1 macrophage polarization, which is regulated by the MAPK/AP-1 pathway, as illustrated in Figure 5D. Ultimately, following the administration of LY294002, the levels of TNF- $\alpha$ , iNOS, and IL-1 $\beta$ , with the exception of IL-6, were notably diminished. This observation implies that JXY facilitates the polarization of M1 macrophages, a process governed by the PI3K/Akt pathway, as depicted in Figure 5E. In summary, JXY fosters the M1-phenotype polarization of RAW264.7 macrophages through the involvement of TLR4 and its downstream NF- $\kappa$ B, MAPK/CREB, MAPK/AP-1, and PI3K/Akt signaling pathways.

## Discussion

CRC is a distressing diagnosis, and its prevalence is progressively increasing over time. The emergence of numerous CRC cases has posed significant challenges to global public health. Conventional treatment modalities, including surgical excision, radiotherapy, and chemotherapy, are susceptible to relapse and exhibit substantial adverse effects.<sup>19,20</sup> Consequently, there is an urgent need for novel approaches to address CRC. JXY, a traditional Chinese medicine, comprises a combination of 4 traditional Chinese medicinal herbs, namely *Hedyotis diffusa* Willd, *Spica Prunellae*, *Pseudobulbus Cremastrae*, and *Sophora Flavescens*. *Hedyotis diffusa* Willd has demonstrated inhibitory effects on the development of CRC by suppressing the proliferation and lymphangiogenesis of CRC cells through the promotion of apoptosis.<sup>21,22</sup> *Spica Prunella* has been substantiated to possess a notable anti-CRC effect, influencing the cell cycle, restraining tumor cell proliferation and angiogenesis, inducing tumor cell apoptosis, and augmenting sensitivity to 5-FU, consequently impeding tumor growth.<sup>23-25</sup> The extract of *Pseudobulbus Cremastrae* has obvious apoptotic effect on HT29 cells of human colon cancer.<sup>26</sup> *Matrine*, a compound derived from *Sophora Flavescens*, has been shown to possess the ability to reverse multiple drug resistances and enhance the sensitivity of chemotherapy drugs.<sup>27</sup> Presently, extensive research is being conducted on the anti-tumor properties of JXY. However, no studies have investigated the impact and underlying mechanism of JXY on macrophage polarization during the progression of CAC. Consequently, this study aims to examine the effects and mechanisms of JXY on macrophage polarization in the development of CAC.

In this study, a CAC mouse model was induced using the AOM/DSS method, which is considered a well-established modeling technique.<sup>28,29</sup> The therapeutic efficacy of JXY on CAC was subsequently assessed. Based on the observation of the overall growth status of the mice, JXY treatment was found to mitigate weight loss, alleviate diarrhea, reduce fecal occult blood, and improve the DAI index in CAC mice. Furthermore, JXY treatment was associated with a decrease in colon length shortening and a reduction in the

number of tumors in CAC mice. Histological examination using H&E staining revealed that JXY treatment ameliorated the pathological structural abnormalities observed in the colon of the model group. These findings provide evidence that JXY exerts inhibitory effects on the development of CAC *in vivo*.

As a complex network of cells, TME are composed of cancer cells, various populations of stromal cells such as infiltrating immune cells (lymphocytes and macrophages), neutrophils, fibroblasts, and signaling molecules. More and more studies have shown a significant association between macrophage polarization and the progression of CRC.<sup>30-32</sup> TAMs possess the ability to inhibit tumor immunity, facilitate tumor growth, invasion, metastasis and drug resistance, ultimately exhibiting a negative correlation with the prognosis of CRC patients.<sup>33</sup> The presence of M2 macrophages, specifically CD68 TAMs, characterized by intense infiltration, is correlated with an unfavorable prognosis and an elevated likelihood of recurrence. These macrophages can induce the expression of numerous cytokines, such as epithelial growth factor (EGF), platelet-derived growth factor (PDGF), and transforming growth factor-beta 1 (TGF- $\beta$ 1), among others. These cytokines facilitate the transmission of signals promoting tumor cell proliferation and survival.<sup>34,35</sup> However, the presence of a substantial number of M1 macrophages confers advantageous outcomes for patients diagnosed with CRC, as it is associated with the elimination of malignant cells via direct mediated cytotoxicity and antibody dependent cell-mediated cytotoxicity (ADCC).<sup>36</sup>

Does JXY inhibit the development of CAC by regulating M1 and M2 macrophages? A study has demonstrated that *matrine*, a main constituent of *Sophora Flavescens*, exhibits the ability to suppress lung cancer metastasis by targeting TAMs polarization, suggesting that the anti-metastatic effects may be attributed to its influence on TAMs polarization.<sup>37</sup> Additionally, *sophoridine*, another major component of *Sophora Flavescens*, has also been observed to inhibit the tumor growth in non-small lung cancer by inducing macrophages M1 polarization through the MAPK-mediated inflammatory pathway.<sup>38</sup> *Oleanolic acid*, a prominent constituent of *Hedyotis diffusa* Willd and *Spica prunellae*, has been shown to inhibit the polarization of macrophages into the M2 phenotype by suppressing STAT3 activation.<sup>39</sup> In our previous investigation, our research team developed self-assembled nanomedical drugs containing *ursolic acid* (UA), another major component of *Hedyotis diffusa* Willd and *Spica prunellae*, and found that UA can repolarize TAMs towards an antitumor M1 phenotype in a CT26 CRC tumor model.<sup>40</sup> These findings suggest that JXY may possess anti-tumor properties through the facilitation of M1 polarization in intestinal mucosal macrophages and the suppression of TAMs formation.

Therefore, an initial investigation was conducted on the M1 and M2 macrophages within the mouse intestinal tissue.



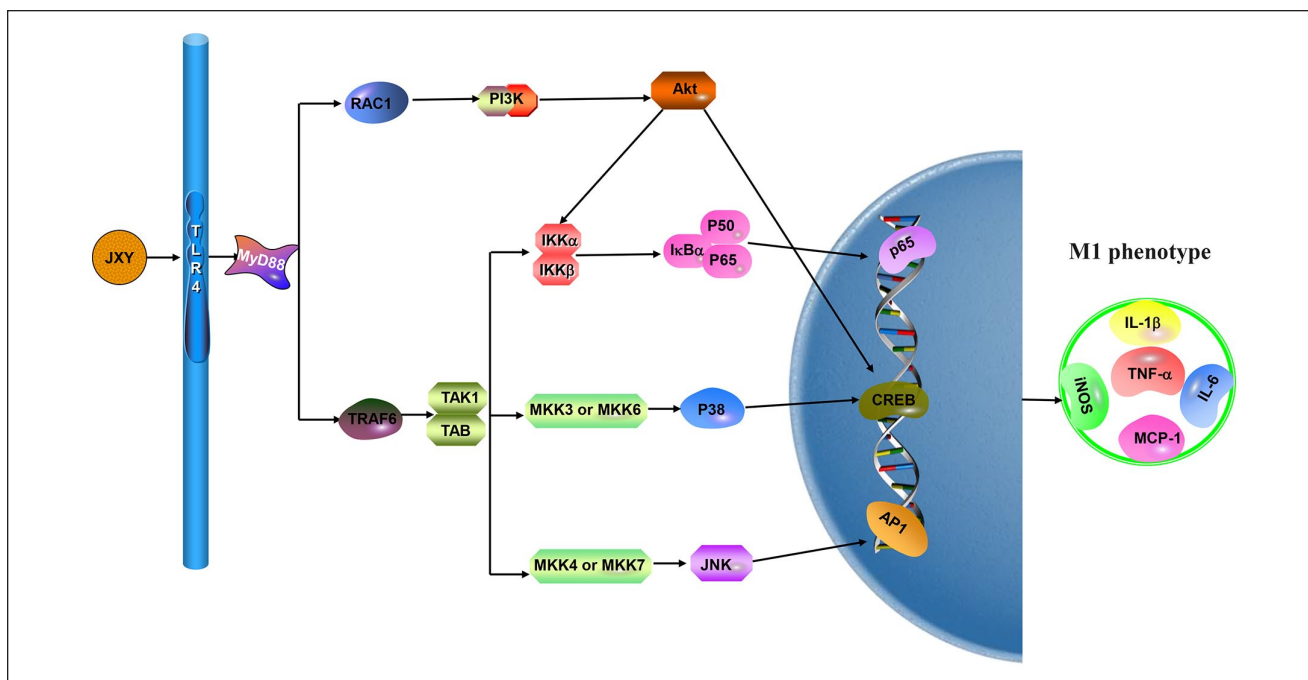


**Figure 6.** The mechanism diagram of JXY promoting M1-type polarization of macrophages.

Immunohistochemistry (IHC) analysis demonstrated that JXY exerts inhibitory effects on the upregulation of total macrophage markers F4/80, CD68, and IBA1 in the murine model, suggesting that JXY may attenuate intestinal inflammation by impeding macrophage infiltration. Meanwhile, JXY was found to enhance the expression of M1 phenotype macrophage markers CD86 and CD11c, while suppressing the expression of M2 phenotype macrophage markers CD206 and Arg-1. These findings suggest that JXY hinders the infiltration of M2 macrophages and promotes the infiltration of M1 macrophages.

In order to provide additional evidence regarding the association between JXY and macrophage polarization, an *in vitro* model of M1 phenotype macrophages was established using RAW264.7 cells. Following intervention with JXY, there was a significant increase in M1 phenotype macrophage-related molecules such as IL-1 $\beta$ , TNF- $\alpha$ , iNOS, as well as co-stimulatory molecules CD80 and CD86. Additionally, the phagocytic capacity of RAW264.7 macrophages was significantly enhanced. These results demonstrate the promotion of M1 macrophage polarization by JXY. Consequently, the investigation proceeded to examine the effects of JXY on M2 phenotype macrophages. Within the TME, the Th2 immune response is known to induce M2 macrophage polarization through the stimulation of IL-4 and IL-13.<sup>11</sup> Therefore, IL-4 was initially employed as an agonist in this study. And it was found that the expression of M2 phenotype macrophage-related molecules Arg-1, CD206, and IL-10 induced by IL-4 was significantly inhibited after JXY intervention. JXY also significantly inhibited

the expression of Arg-1, CD206 and IL-10 in RAW264.7 macrophages cultured with the supernatant of CT26 colorectal cancer cell. The findings suggest that JXY has the ability to suppress the polarization of M2 macrophages within the TME under conditions where Th2 immune response predominates.

At present, the TLR4 pathway exhibits a strong association with M1 macrophage polarization. Upon activation of TLR4, the downstream mediator myeloid differentiation primary response gene 88 (MyD88) is recruited. This recruitment subsequently triggers the downstream activation of tumor necrosis factor receptor-associated protein 6 (TRAF6). Then TRAF6 activates the IKK complex by binding to TGF- $\beta$ -activated kinase (TAK) 1 via TAK1 binding protein (TAB), leading to the induction of the transcription factors nuclear factor (NF)- $\kappa$ B, cAMP response element binding protein (CREB), and activator protein-1 (AP-1). Additionally, TLR4 can activate the Phosphoinositide 3 kinase/Protein kinase B (PI3K/Akt) signaling pathway through MyD88 and TRIF, and also stimulate the transcription factor CREB. The activation of these transcription factors was further promote the release of inflammatory mediators including IL-1 $\beta$ , iNOS, TNF- $\alpha$ , MCP-1, and IL-6, thereby facilitating the formation of M1-phenotype macrophages.<sup>41-44</sup> In order to determine whether JXY's promotion of macrophage polarization to M1 type is regulated by TLR4 and its downstream NF- $\kappa$ B, MAPK/CREB, MAPK/AP-1, and PI3K/Akt signaling pathways, the inhibitors TAK242, PDTC, KG501, SR11302, and LY294002 were utilized. And the results show the effect of JXY on promoting the expression of M1

phenotype macrophage-related molecules was inhibited by these inhibitors, respectively. These findings suggest that JXY facilitates the polarization of M1-type macrophages through the involvement of TLR4 and its downstream signaling pathways, namely NF- $\kappa$ B, MAPK/CREB, MAPK/AP-1, and PI3K/Akt. It is worth noting that the use of the MAPK/AP-1 inhibitor SR11302 resulted in an increase in IL-6 levels, which requires further investigation. Nevertheless, this does not undermine the conclusion that JXY promotes the polarization of macrophages towards the M1 phenotype, which is regulated by the TLR4/MAPK/AP-1 pathway. The regulatory mechanism of JXY promoting M1-type macrophages is shown in Figure 6.

## Conclusion

JXY demonstrates inhibitory effects on CRC development in CAC mice, while also promoting M1 polarization of intestinal mucosal macrophages and inhibiting the formation of TAMs in colon tissues. These effects are attributed to the regulation of TLR4 signaling pathway. This study establishes a fundamental basis for future investigations into the therapeutic potential of JXY in CAC treatment.

## Acknowledgments

Not applicable.

## Availability of Data and Materials

The datasets used and/or analyzed during the current study will be available from the corresponding author upon reasonable request.

## Declaration of Conflicting Interests

The author(s) declared no potential conflicts of interest with respect to the research, authorship, and/or publication of this article.

## Funding

The author(s) disclosed receipt of the following financial support for the research, authorship, and/or publication of this article: This study was supported by the Natural Science Foundation of Fujian Province, China (2020J01747), Chen Ke-Ji Integrative Medicine Development Funds (CKJ2022006), Innovation and entrepreneurship training program for Fujian university students (NO. S202210393028).

## Patient Consent for Publication

Not applicable.

## ORCID iDs

Haiqin Liu  <https://orcid.org/0000-0002-9602-3658>

Ying Lin  <https://orcid.org/0000-0002-1280-2102>

## Supplemental Material

Supplemental material for this article is available online.

## References

1. Sung H, Ferlay J, Siegel RL, et al. Global cancer statistics 2020: GLOBOCAN estimates of incidence and mortality worldwide for 36 cancers in 185 countries. *CA Cancer J Clin.* 2021;70:209-249. doi:10.3322/caac.21660
2. Wu T, Dai Y. Tumor microenvironment and therapeutic response. *Cancer Lett.* 2017;387:61-68. doi:10.1016/j.canlet.2016.01.043
3. Chen H, Zhou H, Li L, et al. Thoughts on the development of TCM oncology. *Chin J Tradit Chin Med Informat.* 2019;26:1-4. (in Chinese)
4. Bai Y, Wei K. Professor Wei Kaijian's experience of using Jiedu Xiaozheng decoction to treat the malignant tumors of Zheng deficiency heat toxin syndrome. *Chin J Ethnomed Ethnopharmacol.* 2022;31:88-92. (in Chinese)
5. Cao Z, Lin W, Huang Z, et al. Jiedu Xiaozheng Yin, a Chinese herbal formula, inhibits tumor angiogenesis via downregulation of VEGF-A and VEGFR-2 expression *in vivo* and *in vitro*. *Oncol Rep.* 2013;29:1080-1086. doi:10.3892/or.2012.2202
6. Cao Z, Chen X, Lin W, et al. Jiedu Xiaozheng Yin decoction inhibits hepatoma cell proliferation by inducing apoptosis via the mitochondrial-mediated pathway. *Mol Med Rep.* 2015;12:2800-2806. doi:10.3892/mmr.2015.3696
7. Hu H, Zheng L, Chen W, et al. Effects of Jiedu xiaozheng decoction on mitochondrial membrane potential and apoptosis in gastric adenocarcinoma cell line BGC-823. *Chin Cancer.* 2010;19:338-342. (in Chinese)
8. Huang Y, Chen W, Hu H, et al. Study on the effect of Chinese compound Jiedu Xiaozheng Yin on apoptosis related genes of gastric carcinoma cells. *Chin Archi Tradit Chin Med.* 2010;28:2143-2147. doi:10.13193/j.archctm.2010.10.129.huangym.058 (in Chinese)
9. Cao Z, Zheng L, Lin W, et al. Jiedu Xiaozheng decoction augments 5-fluorouracil induced anti-hepatic carcinoma effect *in vitro* and *in vivo*. *Rehabilitation Med.* 2019;29:39-46. (in Chinese)
10. Chen X, Li J, Hu D, et al. Jiedu Xiaozheng Yin reverses the resistance of human hepatoma Huh7 cell line to low-dose 5-FU. *Chin J Cell Stem Cell.* 2013;3:191-196. (in Chinese)
11. Lu Q, Guan J, Zeng J, et al. Biological mechanism of Jiedu Xiaozheng Yin in inhibiting hepatocellular carcinoma cell proliferation through regulation of glucose energy metabolism via HIF-1/miR-210 pathway. *Fujian J Tradit Chin Med.* 2022;53:34-41. doi:10.13260/j.cnki.jfjctm.012603 (in Chinese)
12. Shapouri-Moghaddam A, Mohammadian S, Vazini H, et al. Macrophage plasticity, polarization, and function in health and disease. *J Cell Physiol.* 2018;233:6425-6440. doi:10.1002/jcp.26429
13. Zhou D, Huang C, Lin Z, et al. Macrophage polarization and function with emphasis on the evolving roles of coordinated regulation of cellular signaling pathways. *Cell Signal.* 2014;26:192-197. doi:10.1016/j.cellsig.2013.11.004
14. Wang H, Tian T, Zhang J. Tumor-associated macrophages (TAMs) in colorectal cancer (CRC): from mechanism to therapy and prognosis. *Int J Mol Sci.* 2021;22:8470. doi:10.3390/ijms22168470
15. Tacconi C, Ungaro F, Correale C, et al. Activation of the VEGFC/VEGFR3 pathway induces tumor immune escape in colorectal cancer. *Cancer Res.* 2019;79:4196-4210. doi:10.1158/0008-5472.CAN-18-3657

16. Locati M, Curtale G, Mantovani A. Diversity, mechanisms, and significance of macrophage plasticity. *Annu Rev Pathol.* 2020;15:123-147. doi:10.1146/annurev-path-mechdis-012418-012718
17. Sica A, Mantovani A. Macrophage plasticity and polarization: in vivo veritas. *J Clin Invest.* 2012;122:787-795. doi:10.1172/JCI59643
18. Cao Z, Lin W, Huang Z, et al. Ethyl acetate extraction from a Chinese herbal formula, Jiedu Xiaozheng Yin, inhibits the proliferation of hepatocellular carcinoma cells via induction of G0/G1 phase arrest in vivo and in vitro. *Int J Oncol.* 2013;42:202-210. doi:10.3892/ijo.2012.1703
19. Yu H, Hemminki K. Genetic epidemiology of colorectal cancer and associated cancers. *Mutagenesis.* 2020;35:207-219. doi:10.1093/mutage/gez022
20. Xi Y, Xu P. Global colorectal cancer burden in 2020 and projections to 2040. *Transl Oncol.* 2021;14:101174. doi:10.1016/j.tranon.2021.101174
21. Li H, Lai Z, Yang H, et al. Hedyotis diffusa Willd inhibits VEGF-C-mediated lymphangiogenesis in colorectal cancer via multiple signaling pathways. *Oncol Rep.* 2019;42:1225-1236. doi:10.3892/or.2019.7223
22. Lin J, Li Q, Chen H, et al. Hedyotis diffusa Willd extract suppresses proliferation and induces apoptosis via IL-6-inducible STAT3 pathway inactivation in human colorectal cancer cells. *Oncol Lett.* 2015;9:1962-1970. doi:10.3892/ol.2015.2956
23. Lin W, Zheng L, Zhuang Q, et al. Spica Prunellae extract inhibits the proliferation of human colon carcinoma cells via the regulation of the cell cycle. *Oncol Lett.* 2013;6:1123-1127. doi:10.3892/ol.2013.1512
24. Lin W, Zheng L, Zhuang Q, et al. Spica prunellae promotes cancer cell apoptosis, inhibits cell proliferation and tumor angiogenesis in a mouse model of colorectal cancer via suppression of stat3 pathway. *BMC Complement Altern Med.* 2013;13:144. doi:10.1186/1472-6882-13-144
25. Fang Y, Yang C, Zhang L, et al. Spica Prunellae extract enhances fluorouracil sensitivity of 5-fluorouracil-resistant human colon carcinoma HCT-8/5-FU cells via TOP2 $\alpha$  and miR-494. *Biomed Res Int.* 2019;2019:5953619. doi:10.1155/2019/5953619
26. Yu L, Zhai H. Effects of cremastra appendiculata extract on the apoptosis of human colon cancer HT29 cells. *Chin J Ethnomed Ethnopharmacol.* 2016;25:17-19. (in Chinese)
27. Chen MH, Gu YY, Zhang AL, et al. Biological effects and mechanisms of matrine and other constituents of Sophora flavescens in colorectal cancer. *Pharmacol Res.* 2021;171:105778. doi:10.1016/j.phrs.2021.105778
28. Snider AJ, Bialkowska AB, Ghaleb AM, et al. Murine model for colitis-associated cancer of the colon. *Methods Mol Biol.* 2016;1438:245-254. doi:10.1007/978-1-4939-3661-8\_14
29. Parang B, Barrett CW, Williams CS. AOM/DSS model of colitis-associated cancer. *Methods Mol Biol.* 2016;1422:297-307. doi:10.1007/978-1-4939-3603-8\_26
30. Huang C, Ou R, Chen X, et al. Tumor cell-derived SPON2 promotes M2-polarized tumor-associated macrophage infiltration and cancer progression by activating PYK2 in CRC. *J Exp Clin Cancer Res.* 2021;40:304. doi:10.1186/s13046-021-02108-0
31. Qi J, Sun H, Zhang Y, et al. Single-cell and spatial analysis reveal interaction of FAP<sup>+</sup> fibroblasts and SPP1<sup>+</sup> macrophages in colorectal cancer. *Nat Commun.* 2022;13:1742. doi:10.1038/s41467-022-29366-6
32. Zhao S, Mi Y, Guan B, et al. Tumor-derived exosomal miR-934 induces macrophage M2 polarization to promote liver metastasis of colorectal cancer. *J Hematol Oncol.* 2020;13:156. doi:10.1186/s13045-020-00991-2
33. Kasprzak A. The role of tumor microenvironment cells in colorectal cancer (CRC) cachexia. *Int J Mol Sci.* 2021;22:1565. doi:10.3390/ijms22041565
34. Ye L, Zhang T, Kang Z, et al. Tumor-infiltrating immune cells act as a marker for prognosis in colorectal cancer. *Front Immunol.* 2019;10:2368. doi:10.3389/fimmu.2019.02368
35. Edin S, Wikberg ML, Dahlin AM, et al. The distribution of macrophages with a M1 or M2 phenotype in relation to prognosis and the molecular characteristics of colorectal cancer. *PLoS One.* 2012;7:e47045. doi:10.1371/journal.pone.0047045
36. Pan Y, Yu Y, Wang X, et al. Tumor-associated macrophages in tumor immunity. *Front Immunol.* 2020;11:583084. doi:10.3389/fimmu.2020.583084
37. Zhao B, Hui X, Wang J, et al. Matrine suppresses lung cancer metastasis via targeting M2-like tumour-associated-macrophages polarization. *Am J Cancer Res.* 2021;11:4308-4328.
38. Zhao B, Hui X, Zeng H, et al. Sophoridine inhibits the tumour growth of non-small lung cancer by inducing macrophages M1 polarisation via MAPK-mediated inflammatory pathway. *Front Oncol.* 2021;11:634851. doi:10.3389/fonc.2021.634851
39. Fujiwara Y, Takeya M, Komohara Y. A novel strategy for inducing the antitumor effects of triterpenoid compounds: blocking the protumoral functions of tumor-associated macrophages via STAT3 inhibition. *Biomed Res Int.* 2014;2014:348539. doi:10.1155/2014/348539
40. Mao Q, Min J, Zeng R, et al. Self-assembled traditional Chinese nanomedicine modulating tumor immunosuppressive microenvironment for colorectal cancer immunotherapy. *Theranostics.* 2022;12:6088-6105. doi:10.7150/thno.72509
41. Liu L, Guo H, Song A, et al. Progranulin inhibits LPS-induced macrophage M1 polarization via NF- $\kappa$ B and MAPK pathways. *BMC Immunol.* 2020;21:32. doi:10.1186/s12865-020-00355-y
42. Gu X, Zhang Y, Li D, et al. N6-methyladenosine demethylase FTO promotes M1 and M2 macrophage activation. *Cell Signal.* 2020;69:109553. doi:10.1016/j.cellsig.2020.109553
43. Takeda K, Akira S. TLR signaling pathways. *Semin Immunol.* 2004;16:3-9. doi:10.1016/j.smim.2003.10.003
44. Bauerfeld CP, Rastogi R, Pirockinaite G, et al. TLR4-mediated AKT activation is MyD88/TRIF dependent and critical for induction of oxidative phosphorylation and mitochondrial transcription factor A in murine macrophages. *J Immunol.* 2012;188:2847-2857. doi:10.4049/jimmunol.1102157